Enzyme and Microbial Technology 52 (2013) 377–385

Contents lists available at SciVerse ScienceDirect

Enzyme and Microbial Technology

journal homepage: www.elsevier.com/locate/emt

A novel electrochemical biosensor based on horseradish peroxidase immobilized on Ag-nanoparticles/poly(L-arginine) modified carbon paste electrode toward the determination of pyrogallol/hydroquinone

P. Raghu [a], T. Madhusudana Reddy [a,*], K. Reddaiah [a], L.R. Jaidev [b], G. Narasimha [b]

[a] Electrochemical Research Laboratory, Department of Chemistry, S.V.U. College of Sciences, Sri Venkateswara University, Tirupati 517502, Andhra Pradesh, India
[b] Applied Microbiology Laboratory, Department of Virology, Sri Venkateswara University, Tirupati 517502, Andhra Pradesh, India

ARTICLE INFO

Article history:
Received 28 January 2013
Received in revised form 21 February 2013
Accepted 24 February 2013

Keywords:
Horseradish peroxidase
Silica sol–gel
Pyrogallol
Hydroquinone
Carbon paste electrode
Silver nanoparticle

ABSTRACT

A novel electrochemical biosensor for the determination of pyrogallol (PG) and hydroquinone (HQ) has been constructed based on the poly L-arginine (poly(L-Arg))/carbon paste electrode (CPE) immobilized with horseradish peroxidase (HRP) and silver nanoparticles (AgNPs) through the silica sol–gel (SiSG) entrapment. The electrochemical properties of the biosensor were characterized by employing the electrochemical techniques. The proposed biosensor showed a high sensitivity and fast response toward the determination of PG and HQ around 0.18 V. Under the optimized conditions, the anodic peak current of PG and HQ was linear with the concentration range of 8 μM to 30×10^{-5} M and 1–150 μM. The limit of detection (LOD) and limit of quantification (LOQ) were found to be 6.2 μM, 20 μM for PG and 0.57 μM, 1.92 μM for HQ respectively. The electrochemical impedance spectroscopy (EIS) studies have confirmed that the occurrence of electron transfer at HRP-SiSG/AgNPs/poly(L-Arg)/CPE was faster. Moreover the stability, reproducibility and repeatability of the biosensor were also studied. The proposed biosensor was successfully applied for the determination of PG and HQ in real samples and the results were found to be satisfactory.

1. Introduction

Pyrogallol (PG) and hydroquinone (HQ) are derivatives of phenolic compounds which are important contaminants in medical food and environmental matrices. Reliable analytical procedures are required for the determination of PG and HQ in various matrices with high sensitivity. So far, many methods have been developed for their determination, including liquid chromatography [1,2], synchronous fluorescence [3], chemiluminescence [4,5], spectrophotometry [6], gas chromatography/mass spectrometry [7], pH based-flow injection analysis [8], electrochemical methods [9,10], etc., However, most of the above methods have some disadvantages, such as time consuming, high cost, low sensitivity and complicate pretreatment. In recent past, more attention on the development of biosensor was made due to its advantages such as easy preparation, fast detection, low consume of time and high sensitivity [11].

Horseradish peroxidase (HRP) is an important enzyme and is always used as an electron acceptor. Among peroxidases, HRP has been one of the most widely studied enzymes in the development of enzyme based biosensor. Because of the deep embedding of the HRP-active site, which is in unfavorable orientation [12], it is a challenging task to obtain the direct electrochemistry of HRP. According to Marcus theory, the electron transfer (ET) distance is a decisive factor for the direct electrochemistry of redox enzyme, which depends on the overall distance between the redox site within the enzyme and the electrode surface, and the orientation of the enzyme on the electrode [13]. In order to prepare good biosensors, many materials such as nanoparticles, redox dyes, conducting polymers, biomolecules and ionic liquids were employed to improve the microenvironment around the enzyme to provide suitable orientation and to accelerate the electron transfer between the enzyme and the surface of the electrode [11].

Noble metal nanoparticles have been extensively used in the designing and in construction of enzyme biosensors due to their unique characteristics, such as high surface energy and surface to volume ratio, ability to decrease proteins–metal particle distance, good mechanical, thermal and chemical stability [14,15]. So far, the direct electron transfer of HRP has been reported at nanomaterial surfaces such as gold nanoparticles (AuNPs) [16], gold nanowire array electrodes [17], cadmium sulphide [CdS] nanorods [18], and carbon nanotubes (CNTs) [19,20]. The stability and sensitivity of a biosensor could be improved by choosing suitable

* Corresponding author. Tel.: +91 877 2289303.
E-mail addresses: tmsreddysvu@gmail.com, tmsreddy_svu@yahoo.co.in (T. Madhusudana Reddy).

0141-0229/$ – see front matter © 2013 Elsevier Inc. All rights reserved.
http://dx.doi.org/10.1016/j.enzmictec.2013.02.010

enzyme immobilization matrix and by adapting better enzyme immobilization strategies. Recently several valuable immobilization strategies have been employed including absorption [21], cross-linking [22], layer-by-layer assembly [23], sol–gel entrapment [24], electropolymerization [25,26], etc., Among those silica sol–gel (SiSG) entrapment technology has attracted much attention in the field of immobilization of a variety of biomolecules, because of its special features such as chemical inertness, physical rigidity, high-thermal stability, biodegradation and optical transparency [27,28]. However, these HRP-based biosensors require mediators to transfer electrons between the electrode and HRP.

In our previous work, we have developed a biosensor based on the CPE immobilized with HRP, through SiSG entrapment for the determination of hydroquinone (HQ). The electrochemical properties of biosensor were characterized by employing the electrochemical methods like cyclic voltammetry (CV) and differential pulse voltammetry (DPV). The electrocatalytic response of HQ was detected in methanol, ethanol, 2-propoanol, 1-butanol and acetone. The good results were obtained in ethanol as a solvent and acetate buffer solution (ABS) as supporting electrolyte, the experiments were carried out in combination of these two media. The electrochemical impedance spectroscopy (EIS) result confirmed the occurrence of rapid electron transfer at HRP-SiSG/CPE. The proposed sensor was successfully applied for the determination of HQ in real samples and the result were found to be commensurate [29].

In this present work, we have concentrated on embedding HRP into the network of SiSG/AgNPs/poly(L-Arg)/CPE. This technology exhibited a remarkable advantage of AgNPs/poly(L-Arg) and SiSG network. HRP was effectively embedded into the network of AgNPs/poly(L-Arg) which in turn can promote the direct electron transfer of the enzyme immobilized on the electrode surface. The electrocatalytic behavior of this biosensor has also been investigated in detail. The resulting biosensor exhibited high sensitivity and good stability.

2. Experimental

2.1. Reagents

All chemicals were obtained from commercial sources and used without further purification. Horseradish peroxidase (E.C. 1.11.1.7 type-VI-A-S/5 mg, Amoracia rusticana source, 1840 U/mg), pyrogallol and hydroquinone were purchased from Sigma–Aldrich chemicals Co., USA. Tetraethyl orthosilicate (TEOS), cetyltrimethyl ammonium bromide (CTAB), Triton-X-100 were obtained from Sigma–Aldrich chemicals Co., USA. The graphite fine powder was procured from Lobo Chemie and silicon oil from Himedia. Silver nanoparticles (AgNPs) used in the present study were synthesized from fungal culture *Aspergillis niger* and their size (1–3 nm) and shape (spherical) were characterized according to Jaidev and Narasimha [30]. Acetate buffer solution (ABS) was prepared by mixing 0.1 M sodium acetate and 0.1 M acetic acid. All the aqueous solutions were prepared with double distilled water. The enzyme stock solution and working solutions of chemicals were stored in cool place.

2.2. Apparatus

The electrochemical measurements were conducted in a three electrodes cell at a room temperature 25 ± 2 °C. The working electrode was a enzyme immobilized carbon paste electrode (HRP-SiSG/AgNPs/poly(L-Arg)/CPE). The reference electrode was a saturated calomel electrode system and glassy carbon rod electrode was used as an auxiliary electrode. Electrochemical measurements were carried out using CH-Electrochemical Analyzer (Model CHI-660D, CH Instruments, USA).

2.3. Preparation of poly(L-arginine) modified carbon paste electrode (poly(L-Arg)/CPE)

The carbon past electrode was prepared by hand mixing 85% graphite powder and 15% silicon oil in an agate mortar. The carbon paste was then packed into the cavity of a homemade carbon paste electrode with a diameter of 2 mm and smoothed on a weighing paper [31,32]. The 0.038 M of aqueous solution of L-arginine was placed in the electrochemical cell and dipped with CPE and was scanned for eight multiple cycles between the potential ranges from −0.6 V to +1.6 V at 100 mV/s. After polymerization, the poly(L-Arg) film was rinsed sufficiently with double distilled water.

2.4. Fabrication of HRP-SiSG/AgNPs/poly(L-Arg)/CPE

A homogenous TEOS silica sol–gel was prepared by mixing 2 ml of TEOS, 1 ml of H_2O, 50 μl of 0.1 M KCl, 25 μl of 10% Triton-X-100. The mixture was stirred for 1 h for obtaining clear sol. The sol can be stored for about one month when it was kept in refrigerator.

The 5 μl of 5 mg/ml enzyme stock solution was added to the mixture of 5 μl of stock SiSG solution, 40 μl of ABS and 10 μl of AgNPs. A drop of this dispersion with a volume of 5 μl was cast onto the surface of the poly(L-Arg)/CPE, then it was allowed to polymerize at room temperature for 3–5 min. The electrode was gently washed with ABS and was used for further experimental procedure [33]. The 2.5 U of enzyme was immobilized on the electrode surface. The fabrication procedure of the biosensor is illustrated in Scheme 1.

3. Results and discussion

3.1. Electrochemical polymerization of L-arginine on carbon paste electrode

L-Arginine is an amino acid and its electrochemical polymerization potential was between +1.6 V to −0.6 V. The potential window scan lies in the positive direction and this was the most important factor in preparing the poly(L-Arg) film. If the potential window was less than 1.6 V or greater than −0.6 V, it was observed that the formation of poly film on the CPE was not stable. On the other hand, a stable poly film was obtained by the electropolymerization between the potential windows of −0.6 V to +1.6 V and with a maximum of eight cycles on CPE. Fig. 1A shows the growth of polymer film of 0.038 M aqueous L-Arginine solution on the surface of carbon

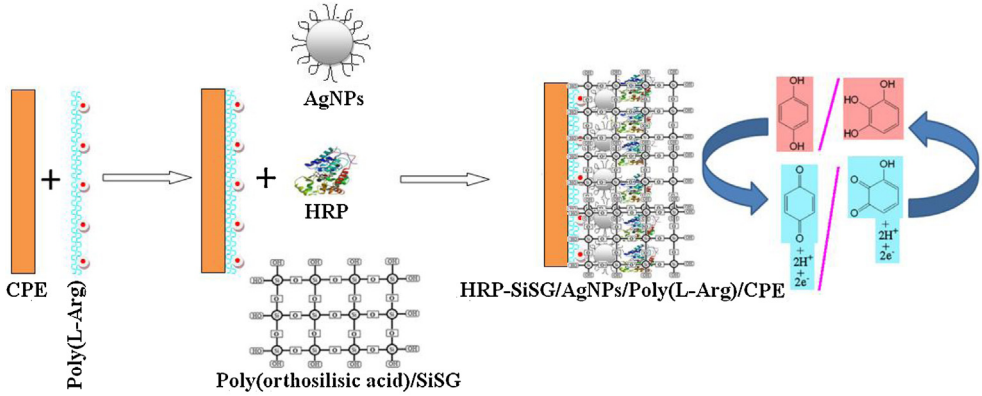

Scheme 1. A schematic diagram showing the steps involved in the fabrication of HRP-SiSG/AgNPs/poly(L-Arg)/CPE with reaction mechanism.

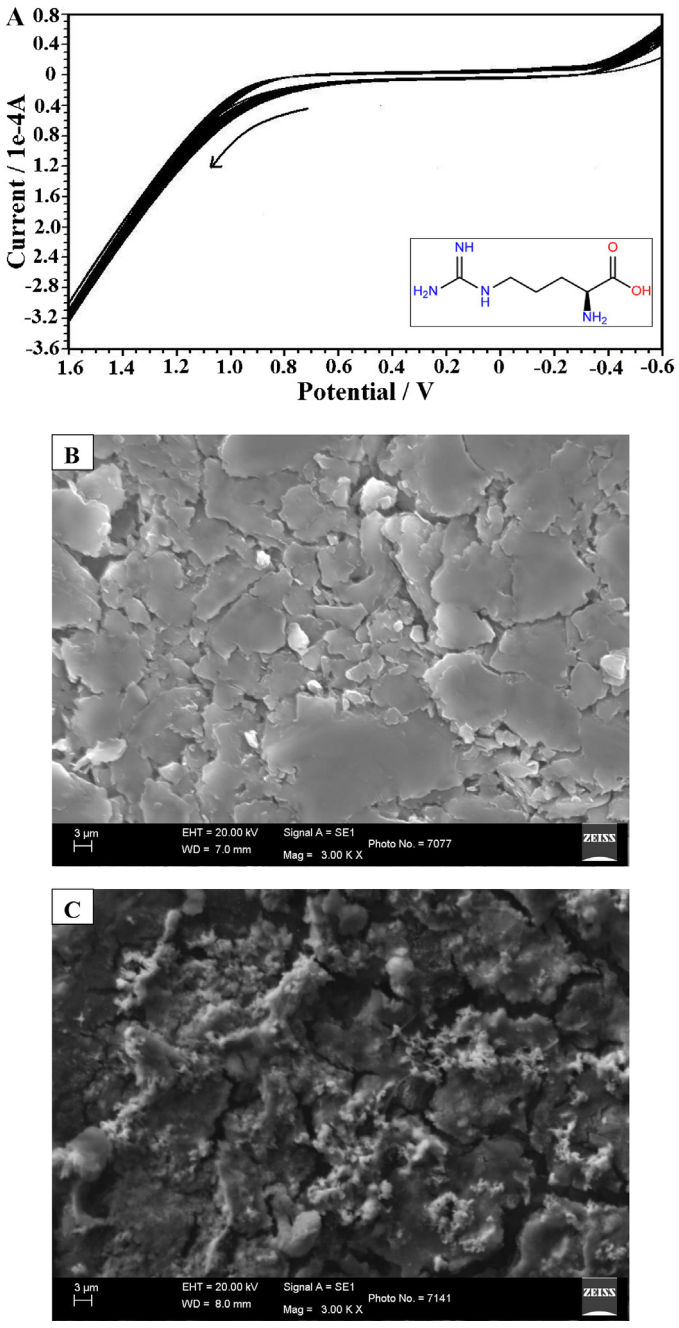

Fig. 1. (A) Cyclic voltammogram for the electrochemical polymerization of (L-arginine) at the carbon paste electrode, inset: structure of L-arginine. SEM images of (B) CPE and (C) HRP-SiSG/AgNPs/poly(L-Arg)/CPE films captured at 3 μM magnifications.

paste electrode. During the process of multiple cycles the voltammogram has gradually descended with increase of cycle time. This indicates that the poly(L-Arg) film was formed and deposited on the surface of carbon paste electrode [34].

3.2. Surface morphological characterizations using scanning electron microscopy (SEM)

SEM study was employed to investigate the surface morphology of bare CPE and HRP-SiSG/AgNPs/poly(L-Arg)/CPE films. The surface of bare carbon paste electrode (bare CPE) was irregularly shaped with 3 μm (3K×) magnification and is shown in Fig. 1B. In this image the flakes of graphite are evenly distributed

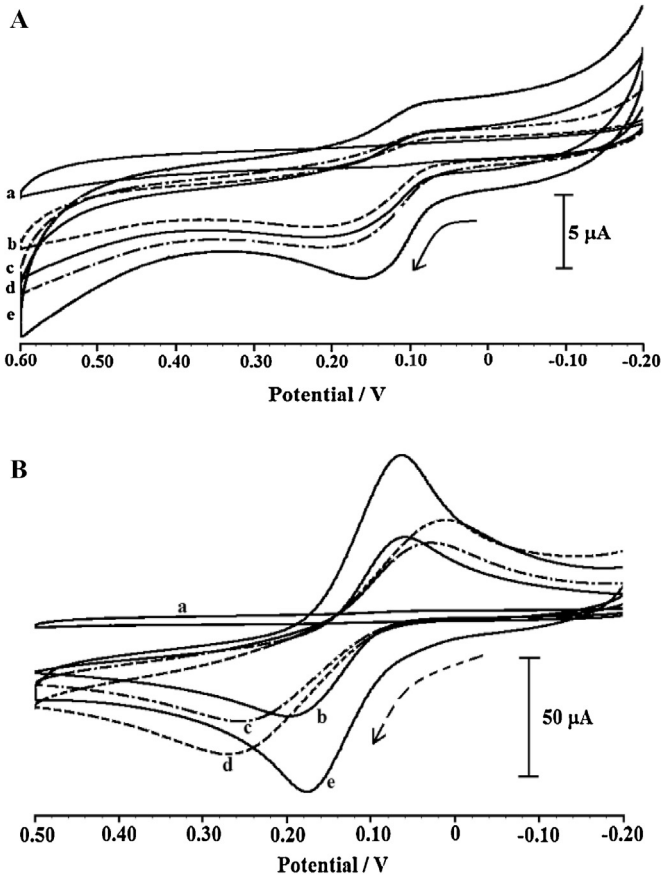

Fig. 2. Cyclic voltammograms of CPE with buffer (a), CPE (b), HRP-SiSG/CPE (c), HRP-SiSG/AgNPs/CPE (d) and HRP-SiSG/AgNPs/poly(L-Arg)/CPE (e) in 1 mM PG/0.1 M ABS (pH 5.0) (A) or in 1 mM HQ/0.1 M ABS (pH 4.5) (B) at a scan rate of 25 mV/s.

throughout the film surface. Fig. 1C shows the SEM image of HRP-SiSG/AgNPs/poly(L-Arg)/CPE with magnification of 3 μm (3K×). Unlike bare CPE film, the enzyme modified CPE film surface posses several bright globular structures, along with uniform and gummy nature background. The SEM results confirmed the formation of HRP-SiSG/AgNPs/poly(L-Arg)/CPE film and clearly demonstrated that AgNPs modified electrode surface is more effective for HRP immobilization.

3.3. Investigation of electrochemical behavior of various film modified CPE's using cyclic voltammetric (CV) studies

The electrochemical behaviors of PG and HQ at the bare CPE, HRP-SiSG/CPE, HRP-SiSG/AgNPs/CPE and HRP-SiSG/AgNPs/poly(L-Arg)/CPE in 0.1 M ABS (pH 5.0/4.5) were studied using CV. Fig. 2A shows the electrochemical responses obtained for the various film modified CPEs in 0.1 M ABS (pH 5.0) with and without 0.1 mM PG. As shown in Fig. 2A no peak was observed at the bare CPE without PG (curve 'a'). When the 0.1 mM PG solution was added, the anodic and cathodic peaks of PG was observed at 0.228 V and 0.069 V at bare CPE (curve 'b'), respectively. The peak potential separation (ΔEp) was about 0.159 V, which indicates that the PG exhibits a quasireversible electrochemical behavior at bare CPE. While at HRP-SiSG/CPE (curve 'c') and HRP-SiSG/AgNPs/CPE (curve 'd'), the peak currents of both anodic and cathodic peaks slightly increases. When it is modified with poly arginine (curve 'e'), there was a good agreement of increase in both anodic and cathodic peak currents, the anodic and cathodic peaks appeared at 0.162 V and 0.079 V respectively with peak to peak separation of 0.083 V. Apart from this, the anodic peak potential decreased from 0.228 to 0.162 V and

the cathodic peak potentials shifted from 0.069 to 0.079 V. These results indicate that the modifiers provide a mimic environment for the functioning of proteins, in which the native conformations of the proteins are retained and the electron transfer rates are greatly enhanced compared with those involving proteins alone at bare electrode [35].

The CV behavior of HQ was also studied at various film modified CPEs under the same conditions, as shown in Fig. 2B. At HRP-SiSG/CPE (curve 'c'), the anodic and cathodic peak potential of HQ appears at 0.255 V and 0.027 V, respectively, with a large ΔEp of 0.228 V. While at HRP-SiSG/AgNPs/poly(L-Arg)/CPE (curve 'e'), the anodic and cathodic peaks appeared at 0.177 and 0.064 V, respectively, with a great reduced in the ΔEp value to 0.113 V. In addition, the anodic and cathodic peak currents were also greatly enhanced. The surface concentration of electroactive HRP (Γ) in HRP-SiSG/AgNPs/poly(L-Arg)/CPE surface was estimated according to following equation [36].

$$Ip = \frac{n^2F^2A\Gamma\nu}{4RT} \quad (1)$$

where Ip is the peak current, A is the electrode active surface area, ν is the scan rate, n is the number of electrons, R, T and F have their usual meanings. By considering the above values, Γ was calculated as 8.63×10^{-8} mol cm^{-2}, which was found to be about 45 times more than the monolayer coverage of HRP (5×10^{-11} mol cm^{-2}) on 3-mercaptopropionic acid modified gold electrode [37]. These results indicated that the multiple layers of active HRP were coated on the electrode surface. The AgNPs/poly(L-Arg)/CPE/SiSG matrix was more efficient for HRP immobilization. The surface concentration of electroactive HRP (Γ) with different immobilization matrices was compared with the present immobilization matrix in Table 1A.

3.4. Effect of solution pH

Fig. 3A and B shows the effect of pH on the electrochemical response of the HRP-SiSG/AgNPs/poly(L-Arg)/CPE toward the determination of PG and HQ respectively. A well defined quasi-reversible redox peaks corresponding to $Fe^{(III/II)}$ redox process of HRP and PG/HQ was observed in the pH range varying from 3.5 to 6.5. The redox peak currents increased with increase in pH of the ABS up to 5.0/4.5 for PG/HQ and thereafter decreased gradually. From these results pH 5.0/4.5 for PG/HQ were selected as the optimum pH values for subsequent experiments. The peak potentials decreases linearly with the increase of pH value and the same is shown in the inset of Fig. 3A and B for PG and HQ respectively. The regression equations between the potential (E) and pH was E (V) = −0.07 pH + 0.5205 (r = 0.9961) for PG and E (V) = −0.052 pH + 0.3694 (r = 0.9798) for HQ. The slopes of potential (E) vs. pH were −70 mV/pH for PG and −52 mV/pH for HQ. These slope values were close to the theoretical slope of (59 mV/pH), which is in accordance with Nernst equation for transfer of equal number of electrons and protons in the reaction [31,32].

3.5. Influence of scan rate

The cyclic voltammograms (CVs) corresponding to various scan rates were also investigated for the fabricated biosensor. Both the anodic and cathodic peak currents increased with increasing potential scan rate. As shown in Fig. 3C and D, a well characterized redox peaks were observed for PG and HQ respectively. Moreover, it was found from the inset of Fig. 3C and D, that the peak currents were proportional to the square root of scan rates, suggesting a typical the semi-infinite linear diffusion-controlled electrochemical behavior feature for both PG and HQ. The catalytic process of HRP-SiSG/AgNPs/poly(L-Arg)/CPE surface toward PG/HQ can be expressed as follows [41].

$$\mathrm{HRP\,(Fe)^{II} + C_6H_7O_3/C_6H_6O_2 \rightarrow Compound\,I\,([Fe^{IV}{=}O]^+) + C_6H_5O_3/C_6H_4O_2} \quad (R1)$$

$$\mathrm{Compound\,I\,([Fe^{IV}{=}O]^+) + e^- + H^+ \rightarrow Compound\,II\,([Fe^{IV}{=}O])} \quad (R2)$$

$$\mathrm{Compound\,II\,([Fe^{IV}{=}O]) + e^- + H^+ \rightarrow HRP\,(Fe^{III}) + H_2O} \quad (R3)$$

Table 1A
Michaelis–Menten constant and Γ values for HRP in different biosensors.

Biosensor	Γ[a]	K_m^{app}[b]	Refs.
HRP/MPA[c]/Au[d]	5×10^{-11} mol cm^{-2}	-	[37]
HRP/nano-Au/ch[e]/GCE[f]	1.2×10^{-9} mol cm^{-2}	1.55 mM	[38]
HRP/DPPA[g]/PGE[h]	1.5×10^{-10} mol cm^{-2}	-	[39]
HRP/colloidal Au/CPE[i]	7.5×10^{-11} mol cm^{-2}	3.69 mM	[40]
HRP/nano-Au/Cys[j]/SiSG[k]/Au	-	1.1 mM	[46]
HRP/colloidal Au/SPCE[l]	-	1.3 mM	[47]
HRP/MB[m]/MWNT[n]/GCE	3.2×10^{-12} mol cm^{-2}	0.12 mM	[48]
CPE/sol–gel-Fer[o]/HRP/sol–gel	-	0.19 mM	[49]
HRP-SiSG/AgNPs[p]/poly(L-Arg)[q]/CPE	8.63×10^{-8} mol cm^{-2}	0.25 mM (for PG)0.11 mM (for HQ)	Present work

[a] Γ, electroactive concentration of HRP on the immobilized electrode surface.
[b] K_m^{app}, apparent Michaelis–Menten constant.
[c] MPA, 3-mercaptopropionic acid.
[d] Au, gold electrode.
[e] ch, choline.
[f] GCE, glassy carbon electrode.
[g] DPPA, dipalmitoylphosphatidic acid.
[h] PGE, pyrolytic graphite electrode.
[i] CPE, carbon paste electrode.
[j] Cys, cysteine.
[k] SiSG, silica sol–gel.
[l] SPCE, screen printed carbon electrode.
[m] MB, methylene blue.
[n] MWNT, multiwalled carbon nanotubes.
[o] Fer, ferrocene.
[p] AgNPs, silver nanoparticles.
[q] Poly(L-Arg), poly(L-arginine).

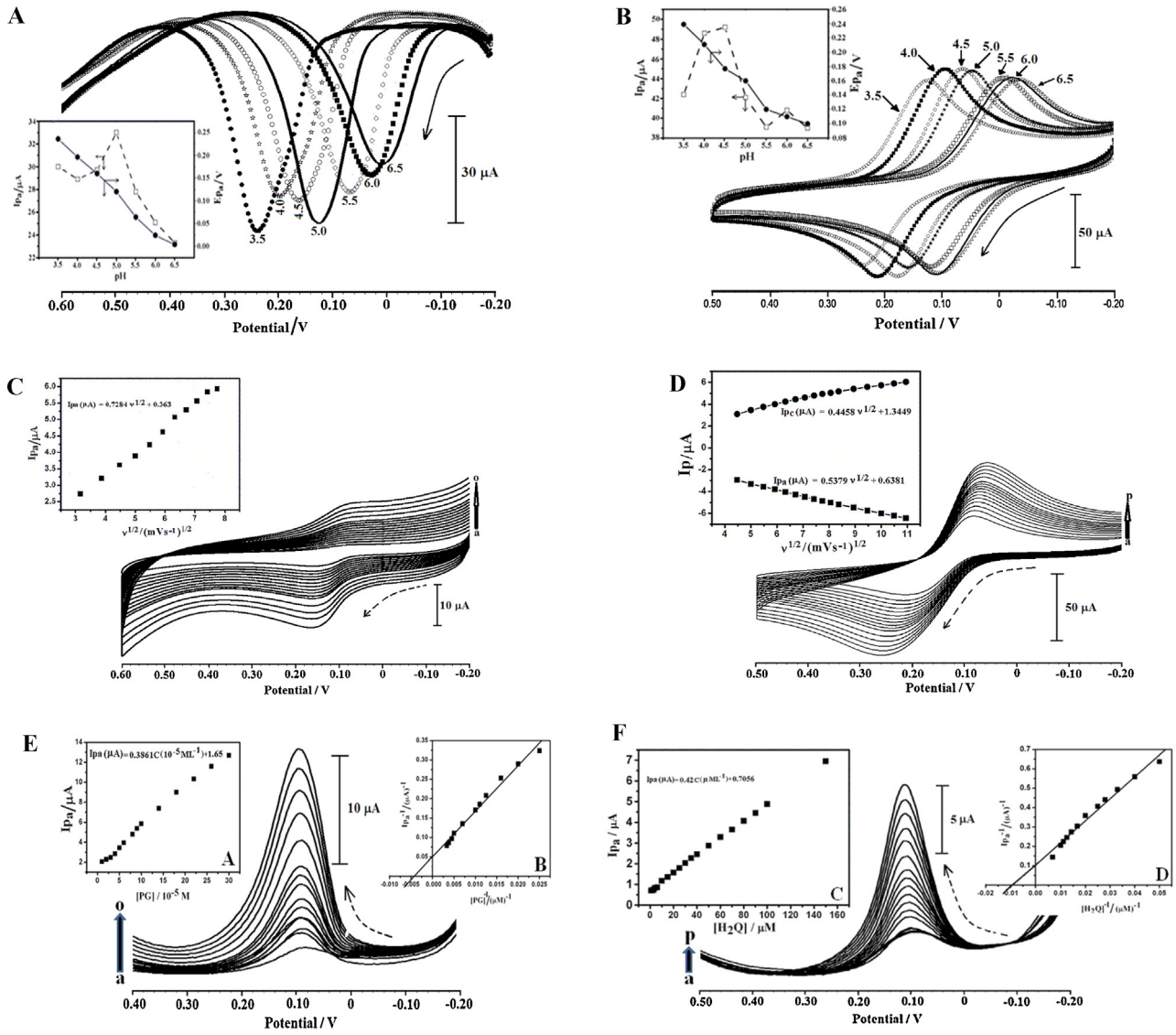

Fig. 3. (A and B) The effect of pH on the redox behavior of HRP-SiSG/AgNPs/poly(L-Arg)/CPE in 0.1 M ABS solution with pH ranging from 3.5 to 6.5 for PG and HQ respectively. The inset is Ip_a/Ep_a vs. pH plot. (C and D) Typical cyclic voltammograms of HRP-SiSG/AgNPs/poly(L-Arg)/CPE and the calibration plot of wave current at different scan rates for 1 mM of PG/0.1 M ABS pH (5.0) ((a) 10 mV/s, (b) 15 mV/s, (c) 20 mV/s, (d) 25 mV/s, (e) 30 mV/s, (f) 35 mV/s, (g) 40 mV/s, (h) 45 mV/s, (i) 50 mV/s, (j) 55 mV/s, (k) 60 mV/s, (l) 70 mV/s, (m) 80 mV/s, (n) 90 mV/s, (o) 100 mV/s) and 1 mM HQ/0.1 M ABS pH (4.5) ((a) 20 mV/s, (b) 25 mV/s, (c) 30 mV/s, (d) 35 mV/s, (e) 40 mV/s, (f) 45 mV/s, (g) 50 mV/s, (h) 55 mV/s, (i) 60 mV/s, (j) 65 mV/s, (k) 70 mV/s, (l) 80 mV/s, (m) 90 mV/s, (n) 100 mV/s, (o) 110 mV/s, (p) 120 mV/s). (E and F) Differential pulse voltammograms of (a) 0.8×10^{-5} M, (b) 1×10^{-5} M, (c) 2×10^{-5} M, (d) 3×10^{-5} M, (e) 4×10^{-5} M, (f) 5×10^{-5} M, (g) 6×10^{-5} M, (h) 8×10^{-5} M, (i) 9×10^{-5} M, (j) 10×10^{-5} M, (k) 14×10^{-5} M, (l) 18×10^{-5} M, (m) 22×10^{-5} M, (n) 26×10^{-5} M, (o) 30×10^{-5} M for PG in 0.1 M ABS (pH 5.0) and (a) 1×10^{-6} M, (b) 3×10^{-6} M, (c) 6×10^{-6} M, (d) 10×10^{-6} M, (e) 15×10^{-6} M, (f) 20×10^{-6} M, (g) 25×10^{-6} M, (h) 30×10^{-6} M, (i) 40×10^{-6} M, (j) 50×10^{-6} M, (k) 60×10^{-6} M, (l) 70×10^{-6} M, (m) 80×10^{-6} M, (n) 90×10^{-6} M, (o) 100×10^{-6} M, (p) 150×10^{-6} M for HQ in 0.1 M ABS (pH 4.5). Inset (A and C) graph of peak current vs. the concentration of PG and HQ respectively. Inset (B and D) Lineweaver–Burk plots for PG and HQ respectively.

3.6. Electrocatalytic determination of PG and HQ at fabricated biosensor

The electrocatalytic activity of HRP-SiSG/AgNPs/poly(L-Arg)/CPE toward PG and HQ was investigated by employing differential pulse voltammetry (DPV) experiment. Fig. 3E and F shows DPV curves for different concentrations of PG/HQ in 0.1 M ABS (pH 5.0/4.5). The results showed that the anodic peak current was proportional to the concentration from 0.8×10^{-5} to 30×10^{-5} M and 1–150 μM for PG and HQ respectively. A good linear relationship was obtained (inset A and C of Fig. 3E and F) with the regression equations of Ip_a (μA) = 0.3861 C (10^{-5} M l^{-1}) + 1.65 (r = 0.9968) for PG and Ip_a (μA) = 0.42 C (μM l^{-1}) + 0.7056 (r = 0.9994) for HQ respectively. The LOD and LOQ of this biosensor were estimated to be 6.2 μM and 20 μM for PG, 0.57 μM and 1.92 μM for HQ respectively. The higher sensitivity of the sensor may result from the good biocompatible microenvironment around the enzyme [42]. The LOD and LOQ values were calculated by using the following expressions [43,44].

$$\mathrm{LOD} = \frac{3S_b}{S} \tag{2}$$

$$\mathrm{LOQ} = \frac{10S_b}{S} \tag{3}$$

where S_b is the standard deviation of mean values for ten differential-pulse voltammograms of blank solution, S is the slope of the working curve.

The apparent Michaelis–Menten constant (K_m^{app}), gives an indication toward the enzyme–substrate kinetics for the biosensor,

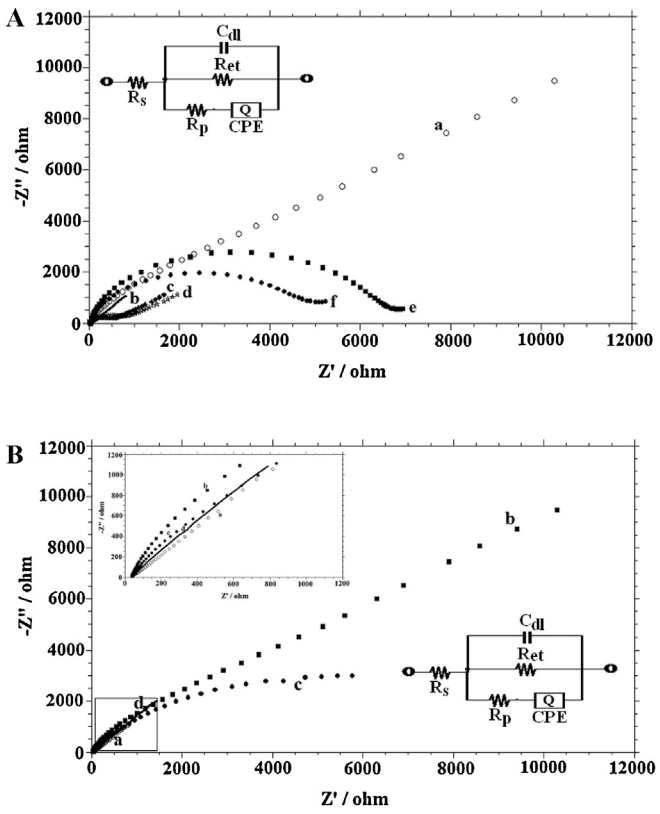

Fig. 4. (A) EIS of (a) bare CPE, (b) HRP-SiSG/AgNPs/poly(L-Arg)/CPE, (c) bare Pt, (d) HRP-SiSG/AgNPs/poly(L-Arg)/Pt, (e) bare GCE, (f) HRP-SiSG/AgNPs/poly(L-Arg)/GCE recorded in 0.1 M KCl containing 1 mM $K_3[Fe(CN)_6]/K_4[Fe(CN)_6]$. Amplitude: 5 mV, frequency: 1 Hz to 100 kHz. (B) EIS of (a) HRP-SiSG/AgNPs/poly(L-Arg)/CPE, (b) bare CPE, (c) CPE/AgNPs, (d) CPE/AgNPs/poly(L-Arg) recorded in 0.1 M ABS pH (4.5)/1 mM $K_3[Fe(CN)_6]/K_4[Fe(CN)_6]$/2 μM of HQ. Amplitude: 5 mV, frequency: 1 Hz to 100 kHz.

and it was calculated from the electrochemical version of the Lineweaver–Burk equation [45].

$$\frac{1}{i_{ss}} = \frac{1}{i_{max}} + \frac{K_m^{app}}{i_{max}C} \quad (4)$$

where i_{ss} is the steady state current after the addition of substrate and i_{max} is the maximum current measured under saturated substrate condition. The K_m^{app} and i_{max} values of the biosensor were found to be 0.25 mM and 20 μA for PG and 0.11 mM and 10 μA for HQ respectively (inset B and D of Fig. 3E and F). Smaller is the K_m^{app} value, higher is the enzyme activity (HRP) and it shows higher affinity toward PG and HQ. The K_m^{app} value of the proposed biosensor was compared with K_m^{app} values of other biosensors in Table 1A.

3.7. Electrochemical impedance spectroscopy (EIS) characterization of biosensor

The EIS is a powerful analytical tool to characterize the electrochemical process occurring at the solution/electrode interface. The curve of the EIS consists of a semicircle portion and a linear portion. At the higher frequencies the semicircle portion was observed, which gives the information of impedance in the form of a diameter. A linear portion was observed at lower frequencies, which represents higher electron transfer. The electron transfer rate at the surface of the electrode was influenced by the surface electron-transfer resistance (R_{et}) of the electrode. Fig. 4A shows the curves of Nyquist plots (Z'' vs. Z') for different types of electrodes. The electrochemical impedance measurements were carried out in 1 mM $K_3[Fe(CN)_6]/K_4[Fe(CN)_6]$ and 0.1 M KCl solution. The alternating voltage was 5 mV and the frequency range was 1 Hz to 100 kHz. It was seen that the bare CPE (a) and HRP-SiSG/AgNPs/poly(L-Arg)/CPE (b) exhibited an almost straight lines, meaning that the probe found it easier to access the surface of the electrode. The Nyquist diameter for bare Pt electrode (c) and bare glassy carbon electrode (GCE) (e) was much larger than that of the corresponding modified HRP-SiSG/AgNPs/poly(L-Arg)/Pt (d) and HRP-SiSG/AgNPs/poly(L-Arg)/GCE (f), which indicates the modified electrodes shows less impedance and more electron transfer rate. The order of impedance for different electrodes was as follows, bare GCE > HRP-SiSG/AgNPs/poly(L-Arg)/GCE > bare Pt > HRP-SiSG/AgNPs/poly(L-Arg)/Pt > bare CPE > HRP-SiSG/AgNPs/poly(L-Arg)/CPE.

Fig. 4B shows EIS results for the different assembly stages of biosensor in 1 mM $K_3[Fe(CN)_6]/K_4[Fe(CN)_6]$ solution prepared by 0.1 M ABS (pH 4.5) and 2 μM of HQ solution. The Randles equivalence circuit model was employed to fit the obtained impedance data, which was shown in inset of Fig. 4B (where R_s represents the solution resistance, C_{dl} is the double layer capacitance, R_{et} is the electron transfer resistance, R_p is the polarization resistance and Q is the CPE (constant phase element)). The curves a–d in Fig. 4B express HRP-SiSG/AgNPs/poly(L-Arg)/CPE (a), bare CPE (b), CPE/AgNPs (c) and CPE/AgNPs/poly(L-Arg) (d) electrodes respectively. According to the curves, 'a' has less impedance (straight line) and the remaining electrodes show slight curve nature. The electron transfer rate constant (K_{et}) values of various electrodes were, bare CPE (0.073 cm/s) < CPE/AgNPs (0.076 cm/s) < CPE/AgNPs/poly(L-Arg) (0.099 cm/s) < HRP-SiSG/AgNPs/poly(L-Arg)/CPE (0.12 cm/s). From the above results it was noticed that the increase in electron transfer rate constant corresponds to the decrease in impedance.

3.8. Stability and reproducibility of biosensor

The fabricated biosensor was continuously tested for 50 successive cycles in the potential range from −0.2 to 0.5 V at the scan rate of 50 mV/s in ABS (pH 4.5/5.0) containing 1 mM PG/HQ. It was noticed that after 50 cycles there was no disturbance in the peak potentials of the system, whereas the peak currents of the system reduced to 88% in comparison with the initial signal. This indicates that the assembly layer was stably fixed on the electrode surface. The results obtained for the developed procedure toward the determination of PG/HQ were reproducible, because there was no significant difference between the RSD values of the both analytes. The results are shown in Table 1B. The long term stability of the HRP-SiSG/AgNPs/poly(L-Arg)/CPE biosensor was investigated under the storage conditions (in a refrigerator, i.e. 4 °C); it was observed that the activity of immobilized HRP was stable up to one month.

Table 1B
The various parameters determined for PG and HQ.

Parameters	PG	HQ
Response time (min)	1	1
Linear range	0.8×10^{-5} to 30×10^{-5} M	1–150 μM
Intercept of calibration curve ($\times 10^{-6}$ A)	1.65	0.7056
Slope of calibration curve ($\times 10^{-6}$ A/M l^{-1})	0.3861	0.42
Correlation coefficient	0.9968	0.9994
Standard deviation of calibration curve	0.2988	0.0611
Limit of detection (LOD)	6.2 μM	0.57 μM
Limit of quantification (LOQ)	20 μM	1.92 μM
Repeatability (%RSD) ($n = 3$)	2.59	3.52
Reproducibility (%RSD) ($n = 3$)	3.14	4.19

n, number of assays.

Table 1C
Recovery results for PG and HQ in spiked samples.

S. No.	Sample matrix	Added (μM)		Found[a] (μM)		Recovery (%)		S.D. (%)		Bias	
		PG	HQ	PG	HQ	PG	HQ	PG	HQ	PG	HQ
1.	Mineralized water	20	20	20.5	19	102	95	0.18	0.12	+2	−5
		40	40	39	41.5	97.5	103	0.21	0.15	−2.5	+3.7
		60	60	61	59	101.6	98	0.17	0.16	+1	−2
2.	Tap water	20	40	21	40.5	105	101	0.16	0.13	+5	+1
		40	60	38	58.5	95	97.5	0.19	0.15	−5	−2.5
		60	80	64	81	106	101	0.18	0.14	+6	+1

[a] Average of four determinations.

Table 1D
Comparison of different electrochemical/other techniques for the determination of HQ and PG.

Electrode	Analyte (linear Conc. range)	Technique	Limit of detection (LOD)	Refs.
GCE[a]	HQ (3.9–1360 μM)	CV[m]	3.9 μM	[50]
	PG (66–440 μM)	CV	33.2 μM	
CNT[b]-GCE	HQ (2.9–1430 μM)	CV	2.9 μM	
	PG (66–1660 μM)	CV	20.0 μM	
HRP[c]-SiSG[d]/CPE	HQ (5–1000 μM)	DPV[n]	1.5 μM	[29]
SiO_2/C[e]	HQ (39–1250 μM)	DPV	1.6 mmol/l	[51]
GCE	HQ (0.5–30 mg/l)	AdSV[o]	50 mg/l	[52]
OMIM-PF6/IL-CPE[f]	HQ (0.01–10 mmol/l)	CV	0.81 mmol/l	[53]
p-(Glu)CPE[g]	HQ (5–80 μM)	DPV	1.5 μM	[54]
SPCE[h]	PG (10–1000 μM)	FIA[p]	0.33 μM	[55]
	PG (75–1000 μM)	LTCC-microchips[q]	75 μM	[56]
Au[i]/CNT/PPY[j]/HRP	PG (1.6–22.4 μM)	CV	1.24 μM	[57]
HRP-SiSG/AgNPs[k]/poly(L-Arg)[l]/CPE	HQ (1–150 μM)	DPV	0.57 μM	Present work
	PG (8–300 μM)	DPV	6.2 μM	

[a] GCE, glassy carbon electrode.
[b] CNT, carbon nano tubes.
[c] HRP, horseradish peroxide.
[d] SiSG, silica sol–gel.
[e] SiO_2/C, silica on carbon electrode.
[f] OMIM-PF6/IL-CPE-1, octyl-3-methylimidazolium-hexafluorophosphate/ionic liquid-carbon paste electrode.
[g] p-(Glu)CPE, poly(Glutamic acid) carbon paste electrode.
[h] SPCE, screen printed carbon electrodes.
[i] Au, gold electrode.
[j] PPY, poly pyrrole.
[k] AgNPs, silver nanoparticles.
[l] Poly(L-Arg), poly(L-arginine).
[m] CV, cyclic voltammetry.
[n] DPV, differential pulse voltammetry.
[o] AdSV, adsorptive stripping voltammetry.
[p] FIA, flow injection amperometry.
[q] LTCC-microchips, fabricated by low temperature co-fired ceramic technique.

3.9. Analytical applications

The practical usage of the biosensor was assessed under optimized conditions by the determination of PG, HQ in the local tap water and mineralized water samples. The spike and recovery experiments were performed through the DPV responses. The amounts of PG/HQ in the tap water/mineralized water samples were determined by calibration method and are summarized in Table 1C. The recoveries were 95–103% and 95–106% for PG and HQ respectively, which clearly indicates the applicability and reliability of the proposed method. The detection limit of various electroanalytical/other methods proposed for the determination of HQ and PG was compared with the present method and shown in Table 1D.

4. Conclusions

In this work, we have successfully developed a method for the determination of PG/HQ by using CV and DPV at HRP-SiSG/AgNPs/poly(L-Arg)/CPE. The method of fabricating the biosensor has many advantages such as ease of fabrication, enhanced electrocatalysis, and long term efficiency in preserving the activity of enzyme molecules. The biosensor exhibited a fast response, a broad liner range, a low detection limit with satisfactory stability, repeatability and good potential application in the determination of PG/HQ in real samples. Attending to these results, the poly(L-Arg)/AgNPs/SiSG matrix was not only a useful tool for facilitating the communication between enzyme and electrode, but also it provides a proper microenvironment for enzyme–substrate interaction.

Acknowledgement

The authors are gratefully acknowledging the financial support from University Grants Commission (UGC), New Delhi, India, in the form of research project no. F. No. 39-709/2010 (SR).

References

[1] Cui H, He CX, Zhao GW. Determination of polyphenols by high-performance liquid chromatography with inhibited chemiluminescence detection. Journal of Chromatography A 1999;855:171–9.

[2] Asan A, Isildak I. Determination of major phenolic compounds in water by reversed phase liquid chromatography after pre-column derivatization with benzoyl chloride. Journal of Chromatography A 2003;988:145–9.
[3] Pistonesi MF, Nezio MSD, Centurion ME, Palomeque ME, Lista AG, Band BSF. Determination of phenol, resorcinol and hydroquinone in air samples by synchronous fluorescence using partial least-squares (PLS). Talanta 2006;69:1265–8.
[4] Cui H, Zhang QL, Myint A, Ge XW, Liu LJ. Chemiluminescence of cerium(IV)–rhodamine 6G-phenolic compound system. Journal of Photochemistry and Photobiology A: Chemistry 2006;181:238–45.
[5] Li SF, Li XZ, Xu J, Wei XW. Flow-injection chemiluminescence determination of polyphenols using luminol–$NaIO_4$–gold nanoparticles system. Talanta 2008;75:32–7.
[6] Nagaraja P, Vasantaha RA, Sunitha KR. A sensitive and selective spectrophotometric estimation of catechol derivatives in pharmaceutical preparations. Talanta 2008;55:1039–46.
[7] Moldoveanu SC, Kiser M. Gas chromatography/mass spectrometry versus liquid chromatography/fluorescence detection in the analysis of phenols in mainstream cigarette smoke. Journal of Chromatography A 2007;1141:90–7.
[8] Garcia-Mesa JA, Mateos R. Direct automatic determination of bitterness and total phenolic compounds in virgin olive oil using a pH-based flow-injection analysis system. Journal of Agricultural and Food Chemistry 2007;55: 3863–8.
[9] Bai J, Guo LP, Ndamanisha JC, Qi B. Electrochemical properties and simultaneous determination of dihydroxybenzene isomers at ordered mesoporous carbon-modified electrode. Journal of Applied Electrochemistry 2009;39: 2497–503.
[10] Yu JJ, Du W, Zhao FQ, Zeng BZ. High sensitive simultaneous determination of catechol and hydroquinone at mesoporous carbon CMK-3 electrode in comparison with multi-walled carbon nanotubes and Vulcan XC-72 carbon electrodes. Electrochimica Acta 2009;54:984–8.
[11] Wang B, Zhang JJ, Pan ZY, Tao XQ, Wang HS. A novel hydrogen peroxide sensor based on the direct electron transfer of horseradish peroxidase immobilized on silica–hydroxyapatite hybrid film. Biosensors and Bioelectronics 2009;24:1141–5.
[12] Zhang WJ, Li GX. Third-generation biosensors based on the direct electron transfer of proteins. Analytical Sciences 2004;20:603–9.
[13] Marcus RA. Electron transfer reactions in chemistry: theory and experiment. Angewandte Chemie International Edition 1993;32:1111.
[14] Pingarron JM, Yanez Sedeno P, Gonzalez-cortes A. Gold nanoparticle-based electrochemical biosensors. Electrochimica Acta 2008;53:5848–66.
[15] Kafi AKM, Ahmadalinezhad A, Wang JP, Thomas DF, Chen AC. Direct growth of nanoporous Au and its application in electrochemical biosensing. Biosensors and Bioelectronics 2010;25:2458–63.
[16] Yin H, Ai S, Shi W, Zhu L. A novel hydrogen peroxide biosensor based on horseradish peroxidase immobilized on gold nanoparticles–silk fibroin modified glassy carbon electrode and direct electrochemistry of horseradish peroxidase. Sensors and Actuators B 2009;137:747–53.
[17] Xu J, Shang F, Luong JHT, Razeeb KM, Glennon JD. Direct electrochemistry of horseradish peroxidase immobilized on a monolayer modified nanowire array electrode. Biosensors and Bioelectronics 2010;25:1313–8.
[18] Zhu Z, Li X, Wang Y, Zeng Y, Sun W, Huang X. Direct electrochemistry and electrocatalysis of horseradish peroxidase with hyaluronic acid-ionic liquid–cadmium sulfide nanorod composite material. Analytica Chimica Acta 2010;670:51–6.
[19] Yang Y, Yang G, Huang Y, Bai H, Lu X. A new hydrogen peroxide biosensor based on gold nanoelectrode ensembles/multiwalled carbon nanotubes/chitosan film-modified electrode. Colloids and Surfaces A 2009;340:50–5.
[20] Wang S, Xie F, Liu G. Direct electrochemistry and electrocatalysis of heme proteins on SWCNTs-CTAB modified electrodes. Talanta 2009;77: 1343–50.
[21] Cao DF, He PL, Hu NF. Electrochemical biosensors utilizing electron transfer in heme proteins immobilised on Fe_3O_4 nanoparticles. Analyst 2003;128:1268–74.
[22] Saroj K, Pradip N. Sunlight-induced covalent immobilization of proteins. Talanta 2007;71:1438–40.
[23] Qu S, Huang F, Chen G, Yu SN, Kong JL. Magnetic assembled electrochemical platform using Fe_2O_3 filled carbon nanotubes and enzyme. Electrochemistry Communications 2007;9:2812–6.
[24] Wang JW, Qu M, Di JW, Gao YS, Wu Y, Tu YF. A carbon nanotube/silica sol–gel architecture for immobilization of horseradish peroxidase for electrochemical biosensor. Bioprocess and Biosystems Engineering 2007;30: 289–96.
[25] Morrin A, Wilbeer F, Ngamna O, Moulton SE, Killard AJ, Wallace GG, et al. Novel biosensor fabrication methodology based on processable conducting polyaniline nanoparticles. Electrochemistry Communications 2005;7:317–22.
[26] Shao Y, Jin YD, Wang JL, Wang L, Zhao F, Dong SJ. Conducting polymer polypyrrole supported bilayer lipid membranes. Biosensors and Bioelectronics 2005;20:1373–9.
[27] Jin W, Brennan JD. Properties and applications of proteins encapsulated within sol–gel derived materials. Analytica Chimica Acta 2002;461:1–36.
[28] Aurobind SV, Amirthalingam KP, Gomathi H. Sol–gel based surface modification of electrodes for electro analysis. Advances in Colloid and Interface Science 2006;121:1–7.
[29] Reddaiah K, Madhusudana Reddy T, Raghu P, Gopal P. Sol–gel immobilized horseradish peroxidase modified carbon paste electrode towards the determination of hydroquinone in non-aqueous solvents: a voltammetric study. Analytical & Bioanalytical Electrochemistry 2012;4:372–85.
[30] Jaidev LR, Narasimha G. Fungal mediated biosynthesis of silver nanoparticles, characterization and antimicrobial activity. Colloids and Surfaces B 2010;81:430–3.
[31] Raghu P, Kumara Swamy BE, Madhusudana Reddy T, Chandrashekar BN, Reddaiah K. Sol–gel immobilized biosensor for the detection of organophosphorous pesticides: a voltammetric method. Bioelectrochemistry 2012;83: 19–24.
[32] Raghu P, Madhusudana Reddy T, Kumara Swamy BE, Chandrashekar BN, Reddaiah K, Sreedhar M. Development of AChE biosensor for the determination of methyl parathion and monocrotophos in water and fruit samples: a cyclic voltammetric study. Journal of Electroanalytical Chemistry 2012; 665:76–82.
[33] Anitha K, Venkata Mohan S, Jayarama Reddy S. Development of acetylcholinesterase silica sol–gel immobilized biosensor – an application towards oxydemeton methyl detection. Biosensors and Bioelectronics 2004;20: 848–56.
[34] Hong Y, Yuanyuan S, Xinhua L, Yuhai T, Liying H. Electrochemical characterization of poly(eriochrome black T) modified glassy carbon electrode and its application to simultaneous determination of dopamine, ascorbic acid and uric acid. Electrochimica Acta 2007;52:6165–71.
[35] Zhang Y, He P, Hu N. Horseradish peroxidase immobilized in TiO_2 nanoparticle films on pyrolytic graphite electrodes: direct electrochemistry and bioelectrocatalysis. Electrochimica Acta 2004;49:1981–8.
[36] Laviron E. The use of linear potential sweep voltammetry and of a.c. voltammetry for the study of the surface electrochemical reaction of strongly adsorbed systems and of redox modified electrodes. Journal of Electroanalytical Chemistry 1979;100:263–70.
[37] Li J, Dong S. The electrochemical study of oxidation-reduction properties of horseradish peroxidase. Journal of Electroanalytical Chemistry 1997;431:19–22.
[38] Zheng Y, Qin LX. Modified electrode based on immobilizing horseradish peroxidase on nano-gold with choline covalently modified glassy carbon electrode as a base. Chinese Journal of Analytical Chemistry 2008;36:604–8.
[39] Liu X, Huang Y, Shang L, Wang X, Xiao H, Li G. Electron transfer reactivity and the catalytic activity of horseradish peroxidase incorporated in dipalmitoylphosphatidic acid films. Bioelectrochemistry 2006;68:98–104.
[40] Liu S, Ju H. Renewable reagentless hydrogen peroxide sensor based on direct electron transfer of horseradish peroxidase immobilized on colloidal gold-modified electrode. Analytical Biochemistry 2002;307:110–6.
[41] Delvaux M, Walcarius A, Demoustier-Champagne S. Electrocatalytic H_2O_2 amperometric detection using gold nanotube electrode ensembles. Analytica Chimica Acta 2004;525:221–30.
[42] Wang BQ, Li B, Deng Q, Dong SJ. Amperometric glucose biosensor based on sol–gel organic–inorganic hybrid material. Analytical Chemistry 1998;70:3170–4.
[43] Madhusudana Reddy T, Reddy SJ. Differential pulse adsorptive stripping voltammetric determination of nifedipine and nimodipine in pharmaceutical formulations, urine, and serum samples by using a clay-modified carbon-paste electrode. Analytical Letters 2004;37:2079–98.
[44] Madhusudana Reddy T, Sreedhar M, Reddy SJ. Voltammetric behavior of Cefixime and Cefpodoxime Proxetil and determination in pharmaceutical formulations and urine. Journal of Pharmaceutical and Biomedical Analysis 2003;31:811–8.
[45] Camacho C, Matías JC, Chico B, Cao R, Gómez L, Simpson BK, et al. Amperometric biosensor for hydrogen peroxide, using supramolecularly immobilized horseradish peroxidase on the β-cyclodextrin-coated gold electrode. Electroanalysis 2007;19:2538–42.
[46] Di J, Shen C, Peng S, Tu X, Li S. A one-step method to construct a third-generation biosensor based on horseradish peroxidase and gold nanoparticles embedded in silica sol–gel network on gold modified electrode. Analytica Chimica Acta 2005;553:196–200.
[47] Xu X, Liu S, Ju H. A novel hydrogen peroxide sensor via the direct electrochemistry of horseradish peroxidase immobilized on colloidal gold modified screen-printed electrode. Sensors 2003;3:350–60.
[48] Xu JZ, Zhu JJ, Wu Q, Hu Z, Chen HY. An amperometric biosensor based on the coimmobilization of horseradish peroxidase and methylene blue on a carbon nanotubes modified electrode. Electroanalysis 2003;15:219–24.
[49] Chut SL, Li J, Tan SN. Reagentless amperometric determination of hydrogen peroxide by silica sol–gel modified biosensor. Analyst 1997;122:1431–4.
[50] Ziyatdinova G, Gainetdinova A, Morozov M, Budnikov H, Grazhulene S, Red'kin A. Voltammetric detection of synthetic water-soluble phenolic antioxidants using carbon nanotube based electrodes. Journal of Solid State Electrochemistry 2012;16:127–34.
[51] Canevari TC, Arenas LT, Landers R, Roxgério C, Gushikema Y. Simultaneous electroanalytical determination of hydroquinone and catechol in the presence of resorcinol at an SiO_2/C electrode spin-coated with a thin film of Nb_2O_5. Analyst 2013;138:315–24.
[52] Niaz A, Sirajuddin Shah A, Mahesar SA, Rauf A. Adsorptive stripping voltammetric determination of hydroquinone using an electrochemically pretreated glassy carbon electrode. Pakistan Journal of Analytical & Environmental Chemistry 2008;9:110–7.
[53] She Y, Tang Y, Liu H, He P. Electrochemical determination of hydroquinone using hydrophobic ionic liquid-type carbon paste electrodes. Chemistry Central Journal 2010;4:17.

[54] Wang L, Huang P, Bai J, Wang H, Zhang L, Zhao Y. Direct simultaneous electrochemical determination of hydroquinone and catechol at a poly(glutamic acid) modified glassy carbon electrode. International Journal of Electrochemical Science 2007;2:123–32.
[55] Feng P-S, Wang S-M, Su W-Y, Cheng S-H. Electrochemical oxidation, sensitive determination of Pyrogallol at Preanodized screen-printed carbon electrodes. Journal of the Chinese Chemical Society 2011;59:1–8.
[56] Goldbach M, Axthelm H, Keusgen M. LTCC-based microchips for the electrochemical detection of phenolic compounds. Sensors and Actuators B 2006;120:346–51.
[57] Korkut S, Keskinler B, Erhan E. An amperometric biosensor based on multiwalled carbon nanotube-poly(pyrrole)-horseradish peroxidase nanobiocomposite film for determination of phenol derivatives. Talanta 2008;76:1147–52.